The Influence of Water Content and Water Dose on Adhesion of Solar Module Interfaces

by

Nicholas Theut

A Thesis Presented in Partial Fulfillment
of the Requirements for the Degree
Master of Science

Approved July 2020 by the
Graduate Supervisory Committee:

Mariana Bertoni, Chair
Zachary Holman
Candace Chan

ARIZONA STATE UNIVERSITY

August 2020

ABSTRACT

Delamination of solar module interfaces often occurs in field-tested solar modules after decades of service due to environmental stressors such as humidity. In the presence of water, the interfaces between the encapsulant and the cell, glass, and backsheet all experience losses of adhesion, exposing the module to accelerated degradation. Understanding the relation between interfacial adhesion and water content inside photovoltaic modules can help mitigate detrimental power losses. Water content measurements via water reflectometry detection combined with 180° peel tests were used to study adhesion of module materials exposed to damp heat and dry heat conditions. The effect of temperature, cumulative water dose, and water content on interfacial adhesion between ethylene vinyl acetate and (1) glass, (2) front of the cell, and (3) backsheet was studied. Temperature and time decreased adhesion at all these interfaces. Water content in the sample during the measurement showed significant decreases in adhesion for the Backsheet/Ethylene vinyl acetate interface. Water dose showed little effect for the Glass/ Ethylene vinyl acetate and Backsheet/ Ethylene vinyl acetate interfaces, but there was significant adhesion loss with water dose at the front cell busbar/encapsulant interface. Initial tensile test results to monitor the effects of the mechanical properties ethylene vinyl acetate and backsheet showed water content increasing the strength of ethylene vinyl acetate during plastic deformation but no change in the strength of the backsheet properties. This mechanical property change is likely inducing variation along the peel interface to possibly convolute the adhesion measurements conducted or to explain the variation seen for the water saturated and dried peel test sample types.

DEDICATION

To Chris and Kelly

ACKNOWLEDGMENTS

I would like to thank all the people responsible for encouraging me and providing me with the resources to learn and grow. I would especially like to thank my parents and grandparents with all their support throughout my education. I would not have been able to pursue my goals without your support and encouragement throughout the years. I would also like to especially thank all of the people in the Defect lab for supporting me initially as an undergraduate and into my Masters degree. The community of people made it easy to get involved when I was an undergraduate and really made me feel included. Everyone was willing to answer all my questions and help me wherever they could. Mariana Bertoni has especially inspired me to push myself and has provided me with wonderful opportunities to learn a variety of areas within photovoltaics.

TABLE OF CONTENTS

Page

LIST OF TABLES

LIST OF FIGURES

CHAPTER 1

INTRODUCTION

Bulk energy production has developed from fuels and resources brought up from the ground, such as oil, natural gas, and coal. Alternative low-carbon emission energy sources have arisen in solar, wind, nuclear, hydro, tidal, and so on. However, as of 2015, renewables consist of less than 25% of worldwide electricity generation [1]. Unfortunately, dependence on carbon-intensive energy sources has led to a plethora of environmental drawbacks including global climate change, ocean acidification, and rising of sea levels [2]. A drive to move away from these fossil fuels has become increasingly important to curb these harmful environmental effects. One of the main alternative energy resources that is widely available for implementation and use is solar photovoltaics. Solar photovoltaics can supply a large portion of these energy needs through continual reductions in levelized cost of energy (LCOE) [3]. Specifically, LCOE can be minimized by reducing PV costs and increasing lifetime power output [3]. Improvements in material reliability and cost are cornerstones of minimizing LCOE [3], [4]. Long-term reliability of PV modules becomes am important facet of this goal within PV. The work presented in this thesis aims to study long-term reliability of PV modules related to water-induced degradation.

1.1 Solar Modules and Field Delamination

Photovoltaic modules—which are exposed to environmental stressors for decades—are routinely warrantied to perform near their maximum power for 20-30 years. Heat, humidity, mechanical strain, and UV radiation are some of the stressors that contribute to power losses through field exposure, with moisture ingress cited as one the largest contributors [5], [6], [7]. Ethylene vinyl acetate (EVA) is the industry go-to encapsulant based on its favorable optical and mechanical properties, as well as relatively low cost [8]. Upon exposure to humidity, heat, and UV radiation, adhesion of EVA to adjacent layers decreases [5], [9], [10]. Delamination within module components is a detrimental degradation process that is promoted by these environmental factors, and occurs most commonly at the interfaces between the polymer encapsulant and i) the front of the cell, and ii) the backsheet [6], [8], [11], [12]. Fig. 1 shows in example of a large area of front cell encapsulant with EVA delaminating from the surface of the front cell [13]. The SEM image clearly shows a separation of the EVA and front cell denoting a delamination failure mechanism [13]. Adhesive failure at the EVA-cell interface exposes the surface

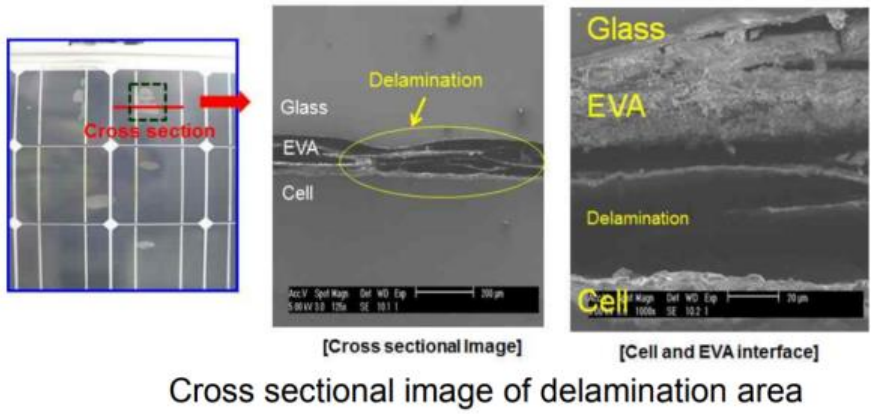

Figure 1: Cross sectional image of delamination area on the front cell of a 5-year field aged PV module in the humid climate conditions of South Korea, figure taken from Park *et al*. [13]

metallization to moisture, resulting in increased corrosion and power losses [8], [14]. This cell adhesion failure occurs in both accelerated damp heat and field-exposed solar modules [5]. Cohesive failure within the bulk EVA has been shown to occur via UV radical and β scission of the ethylene monomers [5], [15]. The backsheet of the module undergoes cracking and tearing as well as adhesive failure with the EVA exposing electrical components within the module to solar cell.

Delamination, cell cracking, and laminate discoloring contribute the most to wear-out failures of modules after reaching the module manufacturer's warranty [16]. These failure types lead to power losses between 0-20% over this warranty period, with delamination seen in more than 80% of the modules of modules analyzed over a 15-year period [16]. However, current material use has begun to reduce some of these delamination and discoloration failures [16]. Yet, delamination continues to be a focus of lessening wear out failures and increasing PV module field lifetimes. It has thus become more important to look at the delamination occurring in currently used EVA, as well as other encapsulants to learn more about the adhesion changes and delamination factors.

1.2 Adhesion Measurements and Related Adhesion Studies

Qunatifying the adheions between photovoltaic module interfaces has thus proven a larger driving factor in finding precise mechanisms for delamination during a module field exposure lifetime and damp heat exposed modules. Several different adhesion measurements have been developed and implemented in testing of PV module materials and in other industries to determine the peel strength and adhesion energy between interfaces. Peel strength is related to the strength during which the interface continually

yields during the adhesion measurement, and it is specific to each measurement type. On the other hand, adhesion energy is more universally distinguished as the energy required to separate the bonds of the material interface, and can be compared acorss techniques. Fig. 2 presents conventional tests that can be used to measure adhesion for the interfaces within a PV module . These include the T-peel test, 90° peel test, 180° peel test, and shear test. Each method can provide slightly variable information and have their benefits and drawbacks. The T-peel test and shear test focus more on the cohesion within the EVA, either at the backsheet or glass interfaces as shown in Fig. 2. They also do not allow for measurements from modules manufactured via standard configuration module configuration. They require an entirely unique sample type. The 180° and 90° allow for

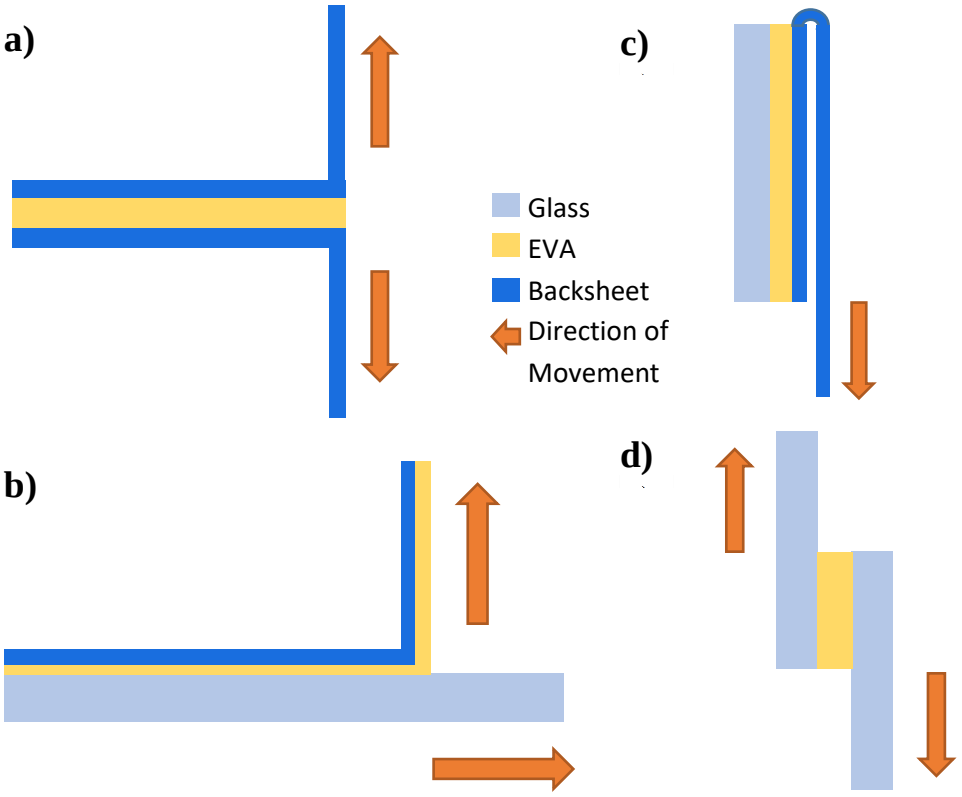

Figure 2: Examples of conventional forms of adhesion measurements including a) T-peel test, b) 90° peel test, c) 180° peel test, and d) shear test

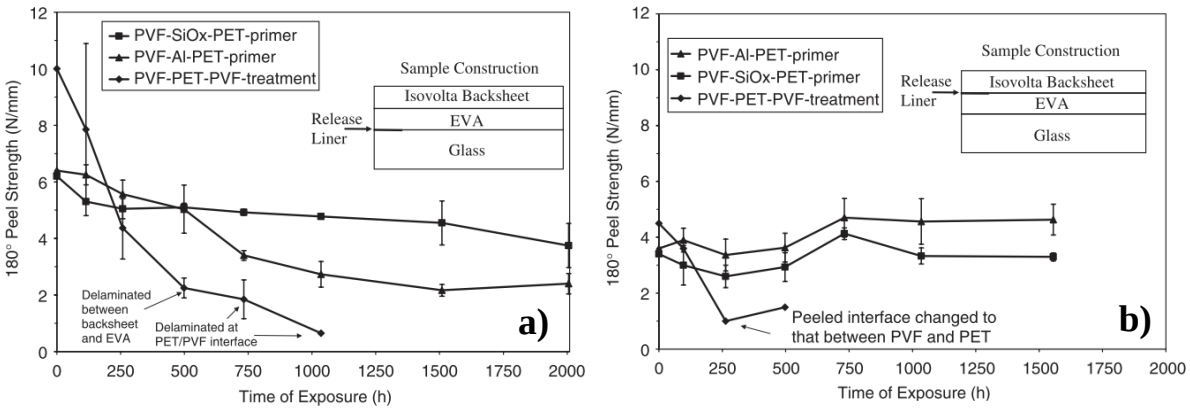

Figure 3 : Previous 180 peel tests conducted by Jorgensen *et al* for a) Glass/EVA and b) Backsheet/EVA interfaces after damp heat exposure [6]

keeping with this more standard configuration seen in module stacks. These 180° and 90° peel tests still include influences from encapsulant cohesion, but to a lesser extent than the T- and shear tests. Thus, adhesion can be more directly measured using these tests. The 90° peel test requires an additional lateral movement of the sample to maintain a consistent vertical peel, making it slightly more complicated to design and implement. The 180° peel test allows for the simplest case setup for less concern about error and provides the opportunity to conduct adhesion measurements at all the relevant module interfaces while manufacturing samples in an architecturcomparable to conventional modules. For the study presented in this work, the 180° peel test is used to measure the interfacial adhesion of solar modules.

Work conducted by Jorgensen *et al.* studied adhesion of different interfaces in PV module materials using a 180° peel test [6]. They observed that at extended damp heat exposure, there was a signfiicant decrease in the peel strength for the Glass/EVA interface.. However, this same decrease in peel strenght was not observed for the Backsheet/EVA interface where there was little to not apparent degradation.

As mentioned above, all of the conventional adhesion measurement tests have limitations, so development of improved techniques has been done subsequently. Most notably, Tracy and colleagues recently developed an improved technique to measure adhesion energy of PV module materials [17]. Fig. 4 a) present their improved adhesion metrology setup and technique through a single cantilever beam [17]. Here, adhesion energies are measured by adhering a titanium beam with a simple triangular geometry, and measuring the force and displacement. This allows for comparative studies to be completed with adhesion energy as the main metric rather than peel strength, which varies considerably between test methods. Fig. 4 b) and c) in particular note the ability for the measurement technique to denote delamination and cohesive failure for EVA within a

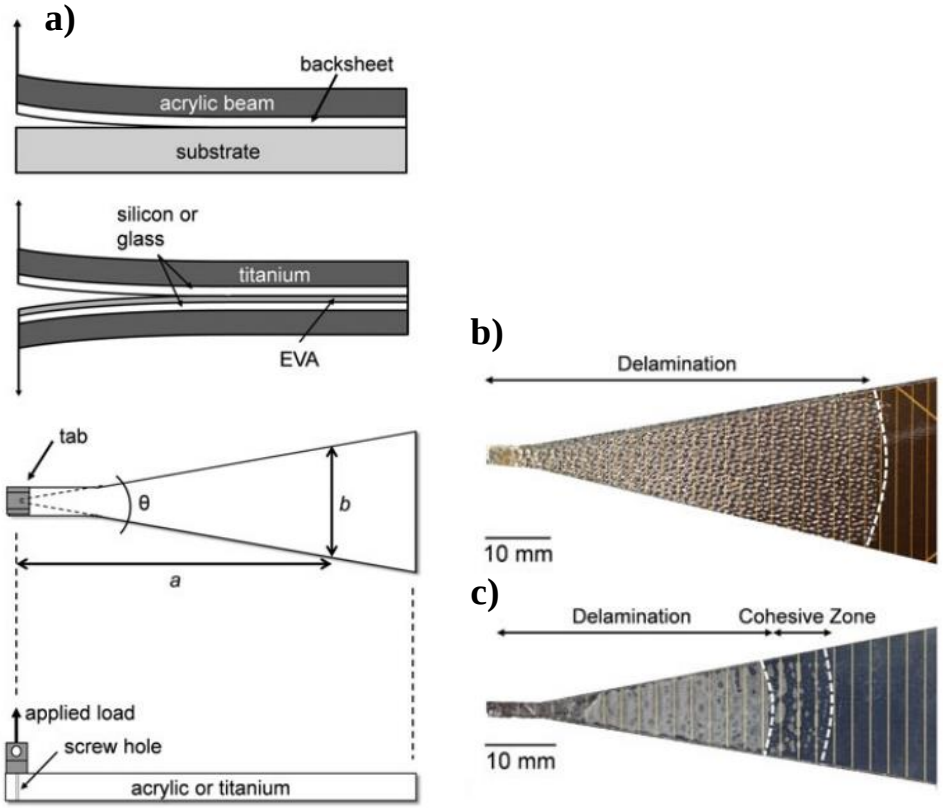

Figure 4: a) An improved adhesion metrology measurement setup by Tracy *et al.* and resulting delamination b) before field exposure and c) after field exposure. Figure taken from [17]**.**

module. In this case, Tracy *et al.* notes that for the field exposed module portion (Fig. 4 c)), there is a significant portion of the area that shows cohesive failure within the module that wasn't observed in the original unexposed module [17]. The ability to easily distinguish between adhesive and cohesive failure in this metrology technique is a notable advantage over those discussed previously. Since this methodology is relatively new and requires custom-built experimental equipment, the work presented in this study uses 180° peel tests. However, this single cantilever beam metrology, is highly valuable and will be used in further future studies beyond the work presented in this thesis.

The single cantilever beam technique has also been used to measure debond energies (also known as adhesion energies). Fig. 5 shows results from an experiment conducted by Bosco *et al.* observing debond energies for the Ag/EVA interface exposed to

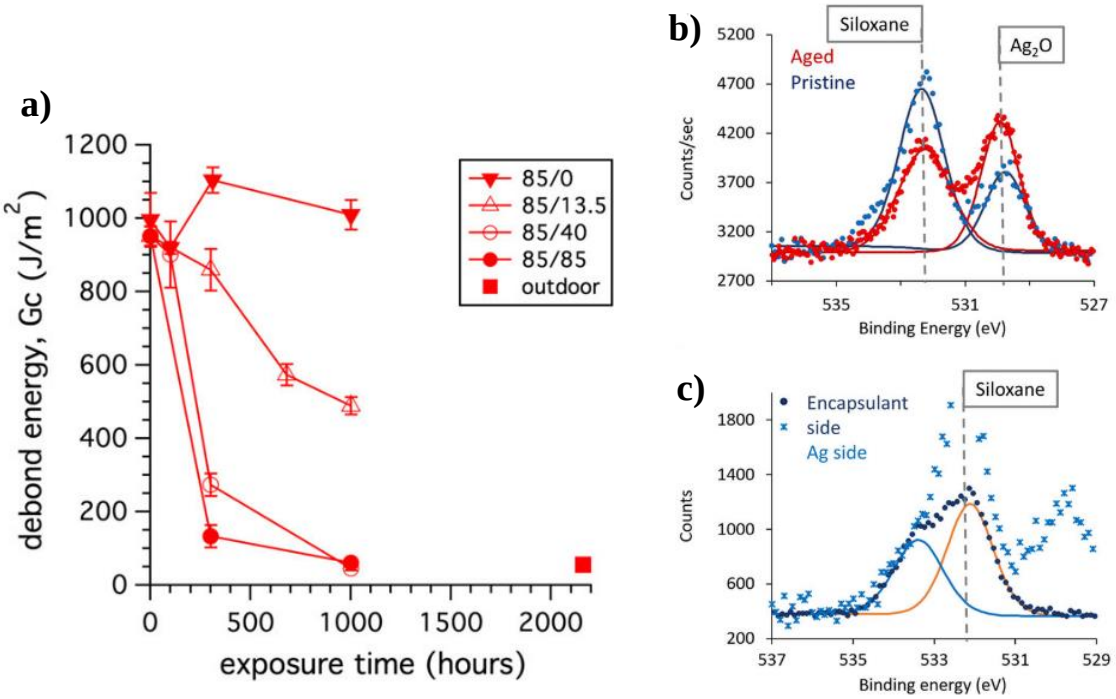

Figure 5: a) Debond energy results from the single cantilever beam test for Ag/EVA interfaces exposed to several conditions and b), c) corresponding chemical products found via XPS measurements found by Bosco *et al.* [18]

several different conditions [18]. The presence of water in the conditions studied was correlated directly to the decreases seen for the debond energies at the Ag/EVA interface, as the dry heat condition (85°C/ 0% RH)showed little to no change in the debond energy over 1000 hours of exposure [18]. They also noted through XPS measurements (Fig. 5 b-c) that there was a reduction in siloxane and an increase in silver oxide. It is stated that the debonding largely occurs at the weakened Ag/EVA interface rather than in "a cohesion fashion within the encapsulant layer" [18]. Furthermore, they investigated further into the nature of the mechanisms working at the Ag/EVA interface in relation to the water exposure [18].

1.3 Ethylene Vinyl Acetate Lamination and Degradation Mechanisms

In the formation of PV modules, ethylene vinyl acetate (EVA) undergoes a crosslinking process by which is strengthens itself and adheres to the other module components. During this crosslinking process, the original thermoplastic polymer transforms itself under heated conditions to a three-dimensional elastomer with a much higher degree of flexibility[19]. EVA also adheres to the modules components and encapsulates the cell as to protect it from the environment. A crosslinker is present inside the EVA to facilitate the crosslinking process, and it is typically an organic peroxide or organic peroxycarboxylic acid [19]. Through a process under temperatures from 120-150 °C, the crosslinker forms radicals on the vinyl acetate branches of the polymer and bonds them together [19]. There are three main factors for this crosslinking process: lamination temperature, lamination time, and initial crosslinker concentration [20]. For the purposes of the study conducted, all three of these conditions were left constant. Lamination was conducted at 145°C for approximately 15 minutes using the same EVA source with the

samples all laminated during the same lamination period. Despite the purpose of EVA to guard the solar cell from environmental stressors after lamination, it is ultimately degraded by these same stressors over years of service.

There are several different mechanisms contributing to the adhesive and cohesive failure with a PV module. Focusing firstly on the Ag/EVA interface, the main mechanism by which the EVA delaminates from the front cell is hydrolytic depolymerization. Hydrolytic depolymerization occurs where the bonded interface of Ag or Si is broken through the presence of water. However, this process of hydrolytic depolymerization occurs very preferentially along the Ag screen printed surface [14]. Work done by Tracy *et al.* has shown that the Ag surface has adhesion energies significantly lower than the antireflective SiN_x coating [14]. It also shows that the Ag surface decreases in adhesion energy far more quickly under 85°C, 85% RH than the SiN_x surface [14]. This preferential delamination about the Ag screen printed interface can be clearly seen in many studies where delamination initiates along the busbar and fingers [14].

Hydrolytic depolymerization reaction also occurs at the Glass/EVA interface. It is largely deduced that this is the primary mechanism by which Jorgensen *et al.* saw a decrease in the Glass/EVA interface during damp heat exposure [21]. There are three other important mechanisms related to delamination and decreased adhesion within photovoltaic modules, these are 1) deacetylation, 2) UV radical generation, and 3) β scission [5]. Fig. 6 shows an illustration of these mechanisms working within a module and their chemical reactions that occur [5]. Fig. 6 also includes information about the kinetics for these reactions as it models them in c) and d). In these models of field-exposed modules, it is clear that the UV radical generation and β scission mechanisms are faster acting

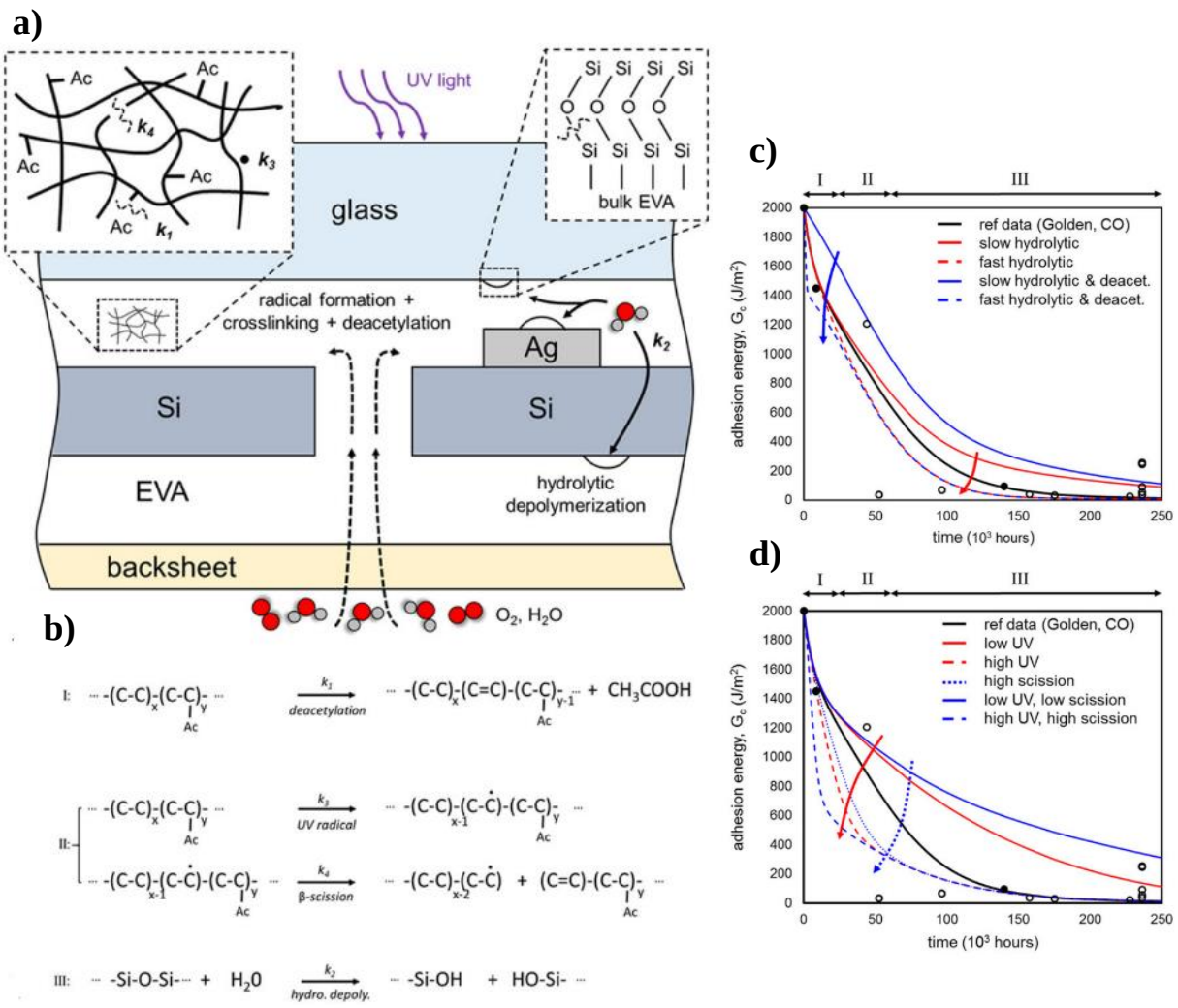

Figure 6: Summary of the processes of encapsulant degradation with an EVA encapsulant with a) a schematic of the module and location of relevant mechanisms, b) chemical reactions for the designated mechanisms of degradation, and simulation results for the sensitivity of the kinetic parameters of the degradation mechanisms for c) hydrolytic depolymerization and deacetylation and d) UV radical generation and β scission reported by Tracy *et al.* [5]

mechanisms for module degradation than deacetylation and hydrolytic depolymerization [5]. This illustrates how these mechanisms might interact and be responsible at different time points within a module's lifetime. Interestingly, hydrolytic depolymerization is a slower a process in field exposed modules, however we expect it to be a dominant degradation mechanism in accelerated damp heat exposures where there are no drying

cycles and no UV irradiation. Since water is a reactant in the process of hydrolytic depolymerization, and moisture ingress is attributed to nearly all degradation modes of PV modules degradation, it is extremely important to directly study the influence of water on interfacial adhesion of module materials [5], [16].

CHAPTER 2

WATER DIFFUSION, WATER DOSE, AND WATER CONTENT

2.1 Experimental Sample Set

Three types of peel test (PT) samples were prepared, one type for each interface in a module; (1) Glass/EVA; (2) Front Cell/EVA; (3) Backsheet/EVA. All PT samples were prepared on 5.1 cm x 5.1 cm glass (McMaster-Carr Borosilicate Glass), with a layer of EVA (3M 9100 EVA), and extended backsheet (Madico PV Backsheet) that acted as a pull-tab for 180° peel tests. When solar cells were included in the PT samples, an adhesive (Krazy Glue) was used to adhere the cells to the glass prior to lamination. To initiate peeling at the desired interface, a Teflon separator (~ 200 µm x 6 cm x 1 cm) was placed between the two layers of interest at the edge starting point of the peel and removed after lamination.

Additionally, a set of samples for was prepared for water content measurements. To mirror the architecture developed for the peel tests, water content (WC) samples were constructed with the same size and EVA thickness. These samples have thin (2-mm-wide) aluminum foil strips between the EVA and backsheet to act as reflective surfaces to

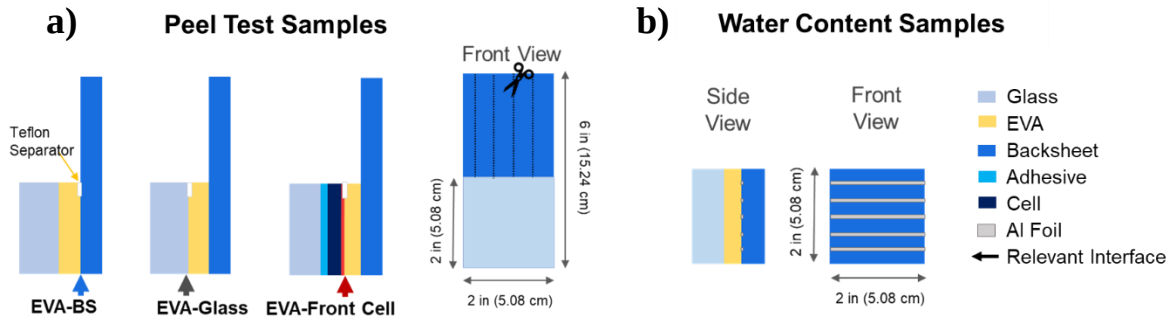

Figure 7: a) Schematics for 180° peel test samples stacks for Backsheet/EVA, Glass/EVA and Front Cell/EVA samples and b) water content sister samples set

measure water content (water content measurements will be described in detail in Section 2.2). All samples (PT and WC) were laminated at 145 °C for approximately 18 minutes using an NPC LM-110x160-S laminator. Sample layers for each set are shown in Fig. 7.

Table 1: Peel Test Experimental Set

Set Name	Experimental Condition	Effect Tested
Wet	85° C, 85%RH - Wet	Water Dose + Water Content +Temperature
Dry	85° C, 85%RH - Dry	Water Dose + Temperature
Reference	85° C, 0%RH	Temperature

2.2 SWIR Water Content Measurements

The water content (WC) sister samples were measured using a technique and tool developed by collaborators using Short Wave Infrared Reflectometry (SWIR). Our collaborators specifically developed this technique for solar modules and designates it as Water Reflectometry Detection, or WaRD technique [22]. This technique uses an infrared laser to detect the presence of water via the change in the normalized amplitude of the O-H water absorption band within EVA about 1902 nm [22]. Fig. 8 shows the specific absorption range that the technique uses and how it calibrates the absorption intensities of the measurement into water concentration inside a solar module. Water content is quantified and mapped with 1 mm x 4 mm spatial resolution throughout the exposure to damp heat (85 °C, 85% RH) and dry heat (85 °C, 0% RH) conditions (see Fig. 9). Following damp heat exposures, the WC samples were measured continually during a water out diffusion period with a sample spatial area being completed every four hours to yield average water concentrations over the module for this same interval. This was

conducted at 85°C and 25 °C to determine out diffusion rates for the Dry and Wet (water saturated) PT samples (see Table I).

2.3 Water Diffusion, Water Dose and Water Content Quantification

To accurately determine the water content and cumulative water dose in the PT samples at the time of the peel test measurements, water out diffusion must be quantified for the Dry and Wet sample sets. Fig. 10 (a) shows the water out diffusion for WC samples at 85 °C after reaching saturation. This was used to determine the duration of drying required to remove the moisture from the Dry PT sample set before conducting peel test

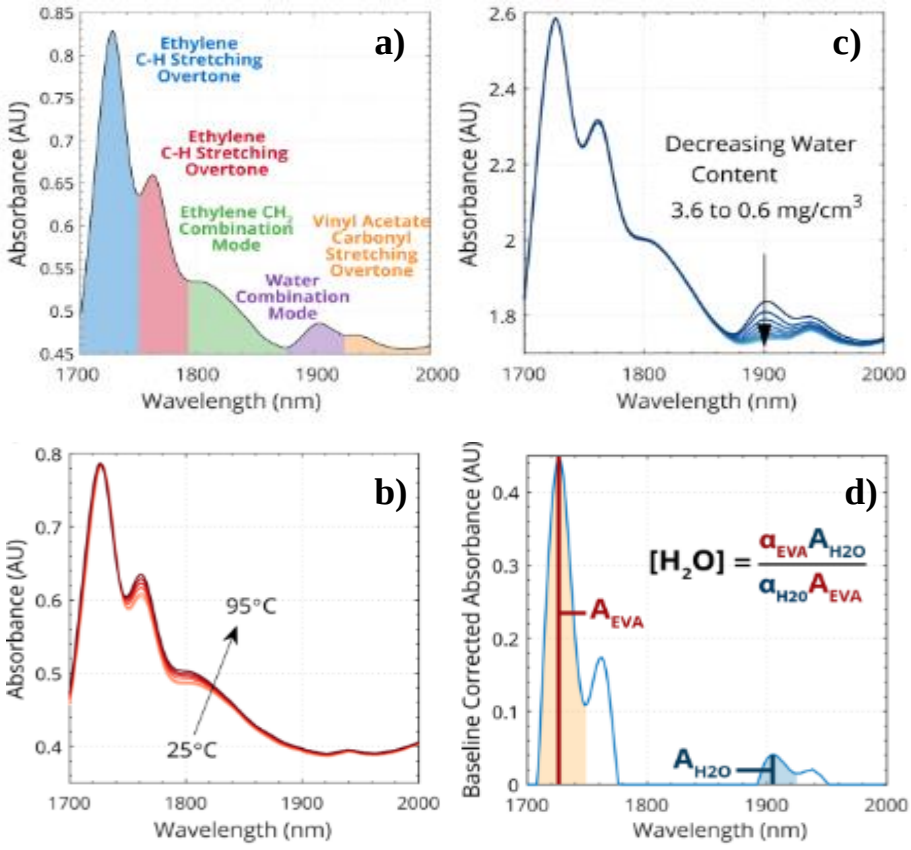

Figure 8: The water and EVA absorption features of interest are labelled in a). The effect temperature on the EVA absorption spectra is shown in b). The absorption spectra for a module saturated with water at 85°C 85%RH is shown in c). The ratio of the peaks shown in d) is used to quantify water content in a module. Figure from Kumar *et al.* [20]

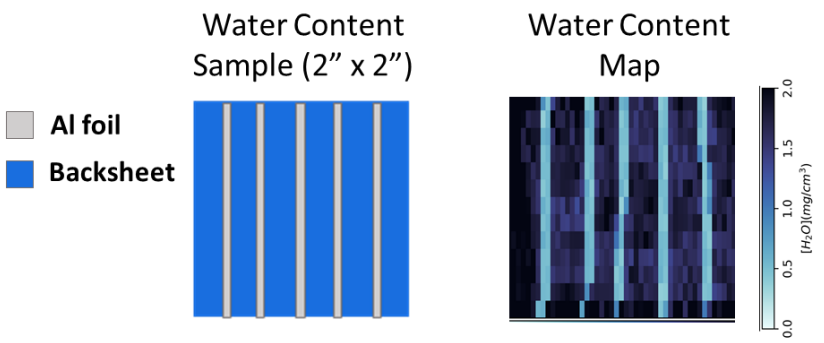

Figure 9: An example of a water content map produced from SWIR over the water content sister samples

measurements. After about 20 h of drying at 85°C, the water content approaches its minimum value at ~ 0.5 mg/cm^3. Therefore, Dry PT samples were dried in the glovebox at 85°C for approximately 24-48 h to ensure complete moisture removal before peel test measurements.

From measurements conducted on 300 h and 700 h WC samples, it is known that the PT samples saturate by 300 h of damp heat exposure. For the Wet PT samples, water begins to out diffuse from the samples immediately following removal from the damp heat chamber. So, the water out diffusion from the time of removal from the damp heat chamber until the time of the peel test measurement needs to be quantified. Fig. 10 (b) shows water out diffusion at 25 °C for WC sisters samples immediately following removal from the damp heat chamber. In this case, the water content measurement remained constant at around 2.25 mg/cm^3 for 8 hours after removal from the damp heat chamber, which is sufficient time to conduct the peel test measurements. However, the WaRD technique cannot evaluate the concentration of condensed water inside the module after cooling the sample from 85 °C to 25 °C. Condensed water could be diffusing from the sample during this time period, but it is undetectable by this measurement technique.

Here, we report the value of 2.25 mg/cm^3 as the water content inside the samples during the PT measurements noting that additional condensed water is also maintained in the sample. Water content measurements conducted continually over the sample out diffusion after damp heat chamber removal did not show large spatial variation as what might be expected between the edge and center of the sample. This is largely in part to the breathable backsheet and high water vapor transmission rate (~ 0.25 mg/cm^2/day). Thus, the following reported water content measurements consider the average value of water over the Al strips across the WC sister samples.

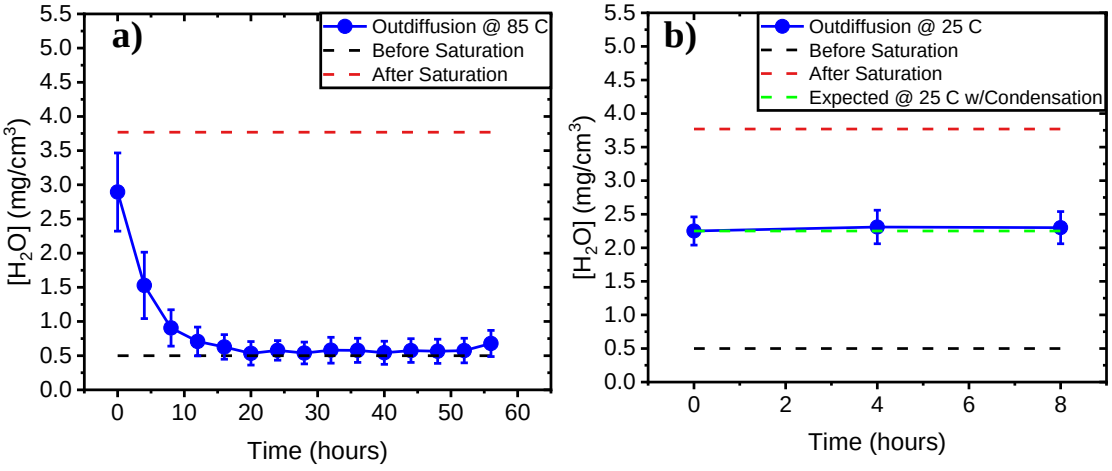

Figure 10: Water out diffusion at a) 85 °C, 60% RH and b) 25 °C, 60% RH for sister water content samples

CHAPTER 3

INTERFACIAL ADHESION AND DEGRADATION STUDIES

3.1 Experimental Setup and Conditions

180° peel tests were performed using an Instron 2530 500 N low profile load cell with a constant peel speed of 10 mm/min. Fig. 11 a) shows the setup for the 180° peel test with the sample mounted in the holder and subsequent peel test conducted as the backsheet is extended peeling the interface. Fig. 12 shows an example of peel forces required for each interface as a function extension. Some peel tests resulted in clean separation of a single interface (shown by shaded boxes in Fig. 12), while other peel tests resulted in convoluted separation of multiple interfaces. This profile is evaluated to determine if the sample had a clean, consistent and successful peel of the desired interface. Fig. 11 b) is an example of what a clean consistent peel would look like, whereas Fig. 11 c) shows a convoluted

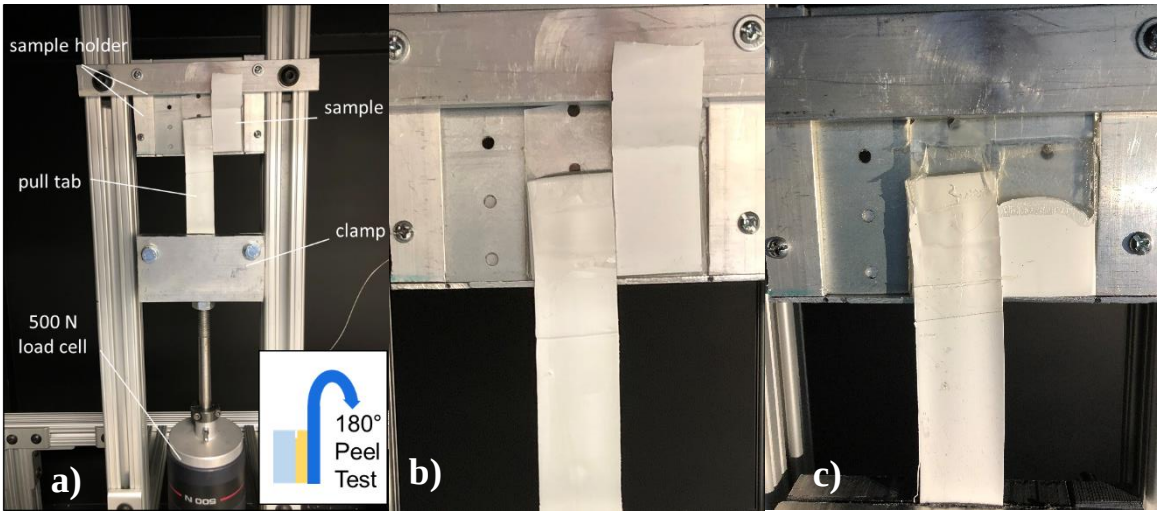

Figure 11: a) 180° peel test experimental setup with sample holder and clamp. b) An example of a clean peel being conducted. c) An example of a convoluted peel.

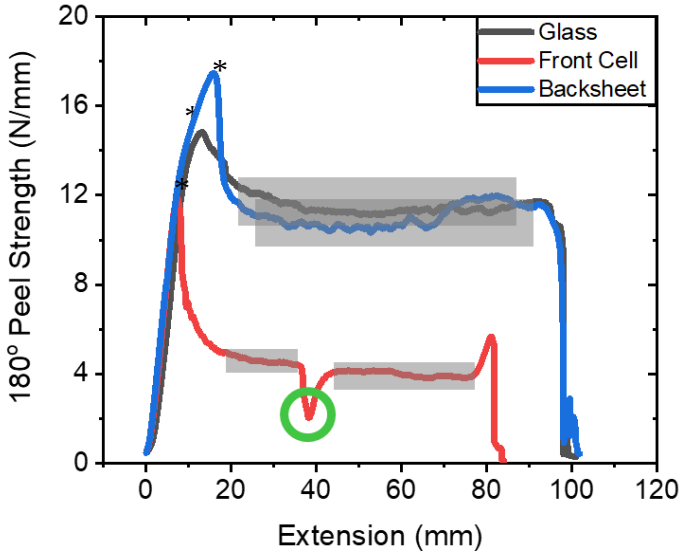

Figure 12: Example data from 180° peel tests after damp heat exposure with the area of interest highlighted for determining the peel force and the green circle indicating the silver busbar on the Front Cell interface.

interface where the Glass/EVA and Backsheet/EVA interfaces are convoluted. Once this is known, an average of the peel force over the indicated extension is calculated to determine the average peel force (see shaded regions in Fig. 12). This peel force is normalized by the width of the backsheet peel tab. Five backsheet peel tabs were used for all peel tests conducted thus far to determine 180° peel strength. The initial peel strength required for initiating separation of the Glass/EVA and Backsheet/EVA interfaces were around 2-3 times greater than Front Cell/EVA interface (as shown by * in Fig. 12). The regions of continuous delamination (shown by the shaded boxes) show similar differences in adhesion strength to the initiation load and are used as the values reported in Section 3.2.

As a recap of the experimental set introduced in Section 2, PT and WC samples were exposed to damp heat (85% RH, 85°C) and dry heat conditions (0% RH, 85°C in a nitrogen filled glovebox). A set of PT samples was exposed to damp heat conditions for 300 h and

700 h. 180° peel tests were conducted within 8 hours of removing the samples from the damp heat chamber; These samples contain water in the sample during the time of the peel test and are thus referred to as the Wet PT samples. Water was confirmed to be still at high concentration in these Wet PT samples by measurements shown in Fig. 11. Furthermore, a set of samples was exposed to the same damp heat conditions, and subsequently dried at 85°C, 0% RH for 20+ hours to remove all water saturated in the sample (see Fig. 11). This set is used to determine the influence on adhesion of cumulative water dose followed by drying. Accordingly, these samples are referred to as the Dry PT samples. The final set, referred to as Reference PT samples, were exposed to 85°C, 0% RH for 300 h and 700 h to separate the temperature and time effects from the water effects. Again, Table 1 in Section 2 summarizes the samples studied in this experiment.

3.2 Interfacical Adhesion Results

After determining the out-diffusion parameters from the WC samples (see Section 2.3), sister PT samples were exposed to the same damp heat and dry heat conditions for the same durations. Fig 13 shows the peel strength for each peel test sample type as a function of water dose and water content. Initial comparison of these results shows the Front Cell/EVA interface has a peel strength ~ 8-10 N/mm lower than the other two interfaces, as expected from earlier initial studies. In Fig. 13, the Backsheet/EVA interface has slightly higher peel strength than its Glass/EVA counterpart. This is in slight contrast to previous work by Jorgensen *et al.* where the Backsheet/EVA interface 180° peel strength was the slightly lower than that for the Glass/EVA interface, possibly due to backsheet improvements and differing lamination conditions [6].

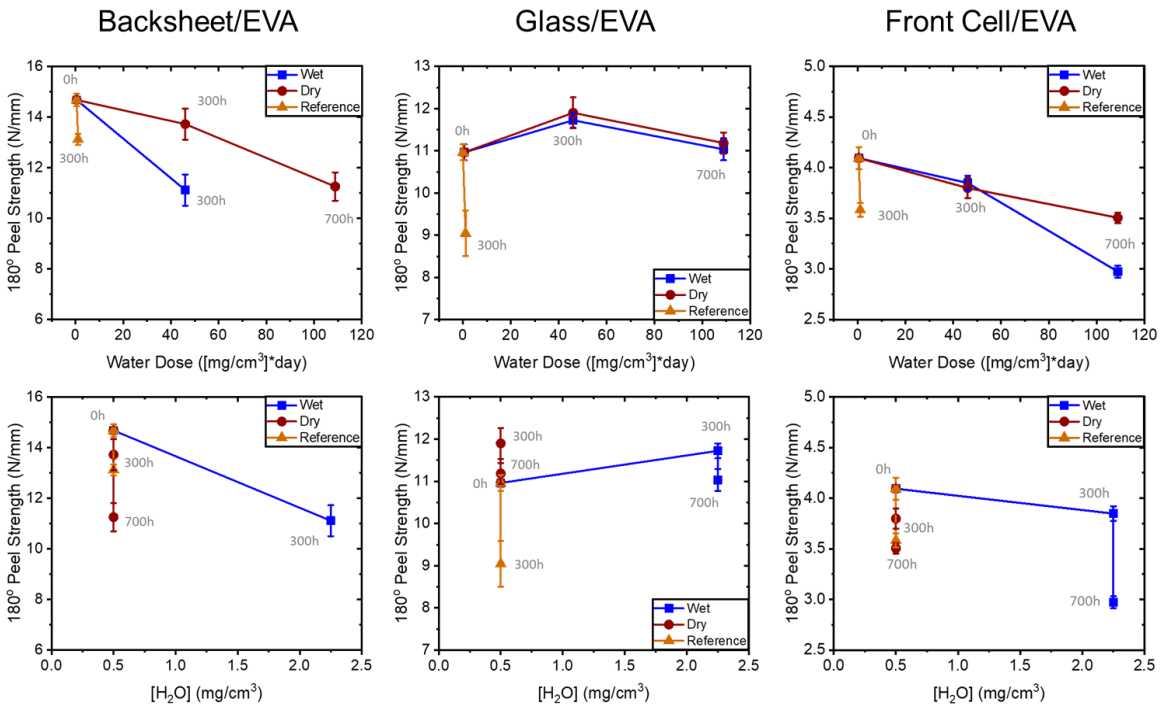

Figure 13: 180° peel strength measurements for Backsheet/EVA, Glass/EVA, and Front Cell/EVA interfaces with corresponding water dose and water content measurements measured inside the samples at 0 h, 300 h, and 700 h of damp heat exposure

For the Backsheet/EVA samples, Fig. 13 shows a decrease in peel strength for all exposure conditions with a notable distinction between the Wet and Dry samples types at 300 h. After the drying, the Dry samples have a peel strength of approximately 2.5 N/mm higher than their Wet counterparts indicating a water content as being a large contributor to adhesion loss at the Backsheet/EVA interface. A similar trend has been reported previously by Jorgensen *et al.* where backsheet/EVA peel test samples exposed to moisture showed that peel strength improved after a 24-hour drying period (with a breathable backsheet) [6]. Similar 180° peel strength magnitudes (~5-15 N/mm) were shown as well by Jorgensen *et al.*, but more substantial adhesion loss was seen in those samples compared to the results in our study [6]. However, the material and processing used were inconsistent likely leading to this separate result. Opposed to water content, water dose does not affect

the peel strength as the Reference and Dry sample types match in peel strength at 300 h indicating temperature and time as larger contributors to this peel strength loss.

The Glass/EVA interface showed largely unexpected results compared to previous literature [6]. Here, the Glass/EVA interface remains relatively constant in peel strength for Wet and Dried samples, but decreases significantly for the Reference sample. A previous report has noted ~2-3 N/mm drops in strength over a similar 700 h damp heat exposures with slightly weaker initial adhesion [6]. The other literature results by Tracy *et al.* have indicated a predominance of the hydrolytic depolymerization mechanism at this interface, where Si-O bonds at the Glass/ EVA interface break down in the presence of water [5]. It has been noted that this mechanism does appear more often at longer field exposure time points, so these early 700 h exposure may not exhibit expected adhesion losses. Water dose and water content do not seem to be as marked factors for this interface in this investigation.

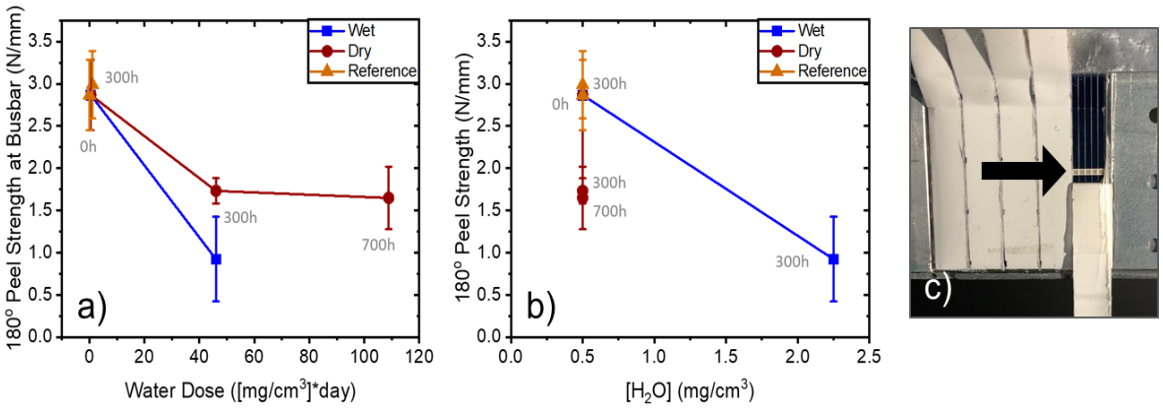

Figure 14: 180° peel strength at the Ag/EVA interface measured over the busbar region of the Front Cell/EVA PT samples with corresponding a) water dose and b) water content measurements after 0 h, 300 h, and 700 h of damp heat exposure. A photo of the busbar region of a Front Cell/EVA PT sample is shown in c).

The Front Cell/EVA interface looks at the influence of adhesion between the EVA, and the silicon nitride bulk (~95% area) and silver finger (~5% area) surface. 180° peel strength decreases for the Wet and Dry samples, but not reduced below the Reference sample. This observation indicates adhesion losses at this interface are more likely influenced by temperature and time rather than water dose or water content. Similar to the Backsheet/EVA interface, there does appear to be a small recovery for the 700 h exposure between the Wet and Dry samples. As this varies from the 300 h case and little-known literature to align this claim, future work will need to be conducted to verify this result to determine if this recovery mechanism to potentially present at this interface. The interface is largely dictated by the silicon nitride surface on the front cell, but silver does contribute separately to a greater degree than the silicon nitride. This can be seen by observing peel strength at the silver busbar during the peel test, shown in Fig. 14. Fig. 14 shows how the peel strength at the Front Cell busbar/EVA interface decreases This agrees with the results from Tracy *et al.* where SiN_x had a significantly higher adhesion energy than the comparable Ag interface, and the Ag interface degraded significantly with damp heat exposure [14]. Fig 14 shows the Ag/EVA interface shows a largely different result than was seen for the larger Front Cell/EVA interface. Fig 14 shows a trend of decreasing peel strength for both the Wet and Dry sample types after 300 h and 700 h damp heat exposure. Yet, the Reference sample did not show any decrease in peel strength at this interface under dry heat conditions. This is a strong indicator that the presence of water over the history of module exposure considerably degrades the interfacial adhesion at this Ag/EVA interface. Contrary to the Glass/EVA interface, this result supports the occurrence of a hydrolytic depolymerization mechanism occurring at this interface, which is one of the notable

mechanisms reported by Tracy *et al.* [5]. Bosco *et al.* has investigated work involving the debonding of the Ag/EVA interface at short humidity timeframes, as was conducted here, and noted a sharp decrease in debond energy with a subsequent plateau [18]. This same phenomenon can be seen here for the Dry sample case where peel strength drops considerably at 300 h with a sustained peel strength afterwards at 700 h. Additionally, there is a slight discrepancy between the Wet and Dry samples at 300 h, which may be indicative of this recovery mechanism discussed previously in the Front Cell/EVA case. The Ag/EVA interface did show results that matched most closely to expectations and reported literature with a large dependence on water dose and sharp decrease at short humidity exposure.

3.3 Intial Tensile Test Results

As the nature of the 180° peel test exposes itself to variation due to the viscoelastic properties of EVA and backsheet, it is important to evaluate how these two materials were independently influenced by moisture. This has been done using a conventional tensile test of the EVA and backsheet laminated independently under comparable conditions to the 180° peel test samples. A comprehensive study of these materials under damp heat exposure has been planned, but at this point, there has been a basic evaluation of the mechanical properties for EVA and backsheet at room temperature with samples at ambient humidity (~30% RH) and at high humidity exposure (~95% RH). The "Wet" samples were exposed to 95% RH at 25°C for 4 hours to introduce a high level of moisture. Precise calculations still need to determine if the samples have achieved complete saturation at this point, but with the particularly small sample dimensions (~0.40 mm thickness, ~6 mm

width). Although the quantity of water is not precisely known, the Wet samples had higher water content than the Dry samples at the time of measurement.

Table 2: EVA and Backsheet Mecahanical Properties with Moisture

Sample Type	Ultimate Tensile Strength (MPa)	Elastic Modulus (GPa)
EVA, Ambient	11 ± 3	0.050 ± 0.005
EVA, Wet	17 ± 2	0.049 ± 0.004
Backsheet, Ambient	114 ± 9	9 ± 1
Backsheet, Wet	116 ± 6	8 ± 1

The samples were measured in the same Intron 500 N load cell used for the 180° peel test studies at 100 mm/min. Following the humidity exposure (95% RH at 25°C for 4 hours), the Wet samples were additionally exposed to moisture using a household humidifier during the tensile test to avoid moisture out diffusion during the measurement. Thus, samples did have a small quantity of condensed water that formed an outer film on the samples. Ten samples were measured for both the Wet and Ambient sets. Table 2 shows the average mechanical properties tested for EVA and backsheet under ambient and water exposure conditions. The ultimate tensile strength for the EVA increased slightly with moisture exposure, but stayed relatively the same for the backsheet. The elastic modulus of the materials did not show significant change with moisture.

Fig. 15 shows the average stress-strain curves for EVA and backsheet before failure. For the EVA curves, the presence of moisture seems to play an important role in increasing the stress required for elongation once plastic deformation is reached in the samples. A higher ultimate tensile strength and curve variation under plastic deformation indicates that water content seems to decrease cohesive failure inside EVA. This

conclusion does not seem to occur for the backsheet, where the curves are very similar. For both EVA and backsheet, the elastic modulus did not show significant change with moisture content and the stress-strain curves in this elastic region are aligned.

Comparing the intial region of backsheet elastic deformation to the 180° peel tests prior to initiation, they show comparable values in terms of elasticity, and it is clear that the backsheet in the 180° peel test does undergo some plastic deformation prior to initation as indicated by the slope change, or yield point, that can be see in Fig 12. However, the subsequent peel strength after the initiation is lower than this yield point, so the backsheet does not continue to undergo the stress required to continue backsheet plastic deformation. Therefore, the backsheet mechanical properties are less likely to influence the 180° peel strength measured after initiation. Yet, it is possible that the yield strength of the backsheet could degrade under damp heat conditions to result in plastic deformation of the backsheet affecting the interface. It is unknown at this point whether this is the case, as future studies are being undergone to look at the EVA and backsheet mechanical properties after

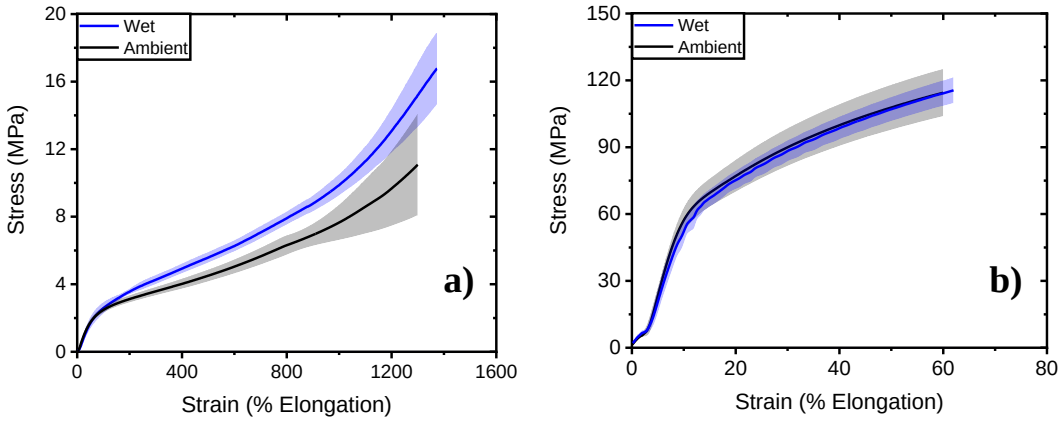

Figure 15: Average stress-strain curves for a) EVA and b) Backsheet after being exposed to ambient and high moisture (Wet) conditions

exposure to 85° C, 85% RH. EVA has a much slower yield point at ~2.5 MPa, which means it does plastically deform under the stresses used to cause continuous peeling during the 180° peel test. It is high likely that the EVA deformation is convoluted within this adhesion measurement. This means the effects of water content with EVA could explain the corresponding recovery mechanism of Wet and Dry PT samples at the Backsheet/EVA interface. Yet, at this point, the mechanism for how this could occur is unknown, as it seems counterinituitive that an increase in the ultimate tensile strength for EVA with water content could lead to a decrease in the 180° peel strength. It is important to note that the adhesion measurements conducted for the Wet and Dry samples was after damp heat exposure, whereas the tensile test samples have yet to experience these conditions. Between EVA and backsheet, EVA is the more likely contributor to 180° peel strength variation.

CHAPTER 4

SUMMARY AND FUTURE WORK

Delamination of solar module interfaces contributes to degradation and limited lifetimes of solar modules. The notable interfaces for delamination are the Glass/EVA, Front Cell/EVA, and Backsheet/EVA interfaces. Moisture is one of the major environmental factors that decrease the adhesion strength of these interfaces. In this study, the water content is measured over damp heat (85°C, 85% RH) exposure using a Water Reflectometry Detection technique (WaRD). 180° peel tests were conducted for samples with this damp heat exposure to determine the adhesion strength of each interface and to correlate this strength with water content inside the EVA. After 700 h of exposure, the Backsheet/EVA interface degraded with temperature and water content present in the EVA but did not show degradation based on the cumulative water dose. The Glass/EVA interface maintained its adhesion in the presence of water, contrary to literature results for adhesion at this interface [6]. However, the Glass/EVA interfacial adhesion deteriorated without water present. Further investigation into this occurrence still needs to be done.

Notably, the lowest peel strength was shown at the Front Cell/EVA interface, where the interface decreased in peel strength for all conditions. Temperature and time were main influencers for this interface with some potential small effects from water content. When considering the silver busbar region at this interface, water dose was a primary factor in decreases in adhesion, as temperature alone did not alter the interfacial adhesion. Outside of this silver interface, all other interfaces showed dependence on temperature, time, and water content rather than water dose.

The initial tensile tests showed that there was a distinct difference between the conditions, where water was highly concentrated in EVA versus the ambient environment. However, water content only had an effect while EVA was undergoing plastic deformation. The EVA undergoes plastic deformation during the 180° peel test measurements. This becomes important to know as the response seen in the 180° peel test is in part due to this viscoelastic property change in EVA. Future investigations are being conducted to complete this understanding of the relation between adhesion and cohesion at these interfaces. These investigations primarily involved comparable damp heat exposure and dry heat exposure timeframes as the PT samples. In addition, proper determination on precise water saturation in these tensile test samples needs to be completed.

In addition to these future tensile tests, some 180° peel test sample sets are also being completed to fill in gaps caused by inconsistent peels and lack of samples at certain conditions. Namely, dry heat (85°C, 0% RH) samples will be conducted at longer durations than 300 h of exposure to compare with damp heat trends. A 25°C, 0% RH set will also be conducted to act as a baseline for aging without temperature as a factor. This is in hope to determine the possible decrease in 85°C, 0% RH for the Glass/EVA interface not seen in the Wet and Dry sample cases. Future studies plan to implement the single cantilever beam method developed by Tracy, Bosco and colleagues to determine the adhesion energies of the interfaces rather than just the 180° peel strength [17]. This measurement technique allows for comparison to new and upcoming literature being presented in PV reliability studies.

Additional studies can help illuminate the trends seen here in this work, but there are some larger takeaways from this that can be applied to PV reliability at large. Firstly,

this study showed the influence of water dose on the Ag/EVA interface. The weakening of this interface and considerably low peel strength indicates that strengthening of this interface is very important for increasing the adhesion inside the module over time. Namely, introducing EVA additives to promote stronger adhesion at this interface or continuing the development of PV sealants could provide the necessary increase in strength or long-term durability. The Backsheet/EVA interface exhibited a weaker strength under high humidity conditions. This might be in part to fluctuating EVA viscoelastic properties, but this is important to note, because the baseline strength of the interface when implemented in higher humidity regions might dispose the module to fail sooner at the interface. The rate of degradation might not change for the interface for as no large change for water dose was seen, rather just a lower baseline strength with higher water content. There are also some concerns about the changes noticed with the EVA during exposure to wet and ambient conditions. The changes in strength and elasticity of EVA between these wet and ambient conditions could lead to internal stresses on the solar cell, leading to crack formation. Additional investigation would need to determine the likelihood of this effect, but it is another failure mechanism that could possible separate from delamination. Lastly, the influence of temperature cannot be stressed enough, as it seemed to be a strong factor throughout the studies with weakening at each interface. Maintaining cooler temperatures on modules would thus mitigate the acceleration of degradation in the cases of acetylation and hydrolytic depolymerization [5].

REFERENCES

[1] M. C. C. de Oliveira, A. S. A. Diniz Cardoso, M. M. Viana, and V. de F. C. Lins, "The causes and effects of degradation of encapsulant ethylene vinyl acetate copolymer (EVA) in crystalline silicon photovoltaic modules: A review," *Renew. Sustain. Energy Rev.*, vol. 81, no. March 2017, pp. 2299–2317, 2018.

[2] I. P. on C. Change, *Climate Change 2014 Synthesis Report*, vol. 9781107025. 2014.

[3] D. B. Needleman, J. R. Poindexter, R. C. Kurchin, I. Marius Peters, G. Wilson, and T. Buonassisi, "Economically sustainable scaling of photovoltaics to meet climate targets," *Energy Environ. Sci.*, vol. 9, no. 6, pp. 2122–2129, 2016.

[4] A. Feltrin and A. Freundlich, "Material considerations for terawatt level deployment of photovoltaics," *Renew. Energy*, vol. 33, no. 2, pp. 180–185, 2008.

[5] J. Tracy, D. R. D'hooge, N. Bosco, C. Delgado, and R. Dauskardt, "Evaluating and predicting molecular mechanisms of adhesive degradation during field and accelerated aging of photovoltaic modules," *Prog. Photovoltaics Res. Appl.*, vol. 26, no. 12, pp. 981–993, 2018.

[6] G. J. Ã. Jorgensen *et al.*, "Moisture transport , adhesion , and corrosion protection of PV module packaging materials," *Sol. Energy Mater. Sol. Cells*, vol. 90, no. 16, pp. 2739–2775, 2006.

[7] M. D. Kempe, G. J. Jorgensen, K. M. Terwilliger, T. J. McMahon, C. E. Kennedy, and T. T. Borek, "Ethylene-vinyl acetate potential problems for photovoltaic packaging," *Conf. Rec. 2006 IEEE 4th World Conf. Photovolt. Energy Conversion, WCPEC-4*, vol. 2, pp. 2160–2163, 2007.

[8] M. D. Kempe, G. J. Jorgensen, K. M. Terwilliger, T. J. McMahon, C. E. Kennedy, and T. T. Borek, "Acetic acid production and glass transition concerns with ethylene-vinyl acetate used in photovoltaic devices," *Sol. Energy Mater. Sol. Cells*, vol. 91, no. 4, pp. 315–329, 2007.

[9] S.-Y. Kook and R. H. Dauskardt, "Moisture-assisted subcritical debonding of a polymer/metal interface," *J. Appl. Phys.*, vol. 91, no. 3, pp. 1293–1303, 2002.

[10] A. Badiee, I. A. Ashcroft, and R. D. Wildman, "The thermo-mechanical degradation of ethylene vinyl acetate used as a solar panel adhesive and encapsulant," *Int. J. Adhes. Adhes.*, vol. 68, pp. 212–218, 2016.

[11] W. Oh *et al.*, "The degradation of multi-crystalline silicon solar cells after damp heat tests," *Microelectron. Reliab.*, vol. 54, no. 9–10, pp. 2176–2179, 2014.

[12] M. D. Kempe, “Modeling of rates of moisture ingress into photovoltaic modules,” *Sol. Energy Mater. Sol. Cells*, vol. 90, no. 16, pp. 2720–2738, 2006.

[13] N. Park, C. Han, W. Hong, and D. Kim, “The effect of encapsulant delamination on electrical performance of PV module,” *Conf. Rec. IEEE Photovolt. Spec. Conf.*, pp. 001113–001115, 2011.

[14] J. Tracy, N. Bosco, and R. Dauskardt, “Encapsulant Adhesion to Surface Metallization on Photovoltaic Cells,” *IEEE J. Photovoltaics*, vol. 7, no. 6, pp. 1635–1639, 2017.

[15] M. Gagliardi, P. Lenarda, and M. Paggi, “A reaction-diffusion formulation to simulate EVA polymer degradation in environmental and accelerated ageing conditions,” *Sol. Energy Mater. Sol. Cells*, vol. 164, pp. 93–106, 2017.

[16] M. Köntges *et al.*, *Review of Failures of Photovoltaic Modules*. 2014.

[17] J. Tracy, N. Bosco, F. Novoa, and R. Dauskardt, “Encapsulation and backsheet adhesion metrology for photovoltaic modules,” *Prog. Photovoltaics Res. Appl.*, vol. 25, no. 1, pp. 87–96, 2017.

[18] N. Bosco, S. Moffitt, and L. T. Schelhas, “Mechanisms of adhesion degradation at the photovoltiac module ’ s cell metallization - encapsulant interface,” *Prog. Photovoltaics Res. Appl.*, vol. 27, no. August 2018, pp. 340–345, 2019.

[19] C. Hirschl *et al.*, “Determining the degree of crosslinking of ethylene vinyl acetate photovoltaic module encapsulants - A comparative study,” *Sol. Energy Mater. Sol. Cells*, 2013.

[20] C. Hirschl *et al.*, “In-line determination of the degree of crosslinking of ethylene vinyl acetate in PV modules by Raman spectroscopy,” *Sol. Energy Mater. Sol. Cells*, vol. 152, pp. 10–20, 2016.

[21] M. D. Kempe, G. J. Jorgensen, K. M. Terwilliger, T. J. Mcmahon, C. E. Kennedy, and T. T. Borek, “Acetic acid production and glass transition concerns with ethylene-vinyl acetate used in photovoltaic devices,” *Sol. Energy Mater. Sol. Cells*, vol. 91, no. 4, pp. 315–329, 2007.

[22] R. E. Kumar, G. Von Gastrow, J. Leslie, R. Meier, M. I. Bertoni, and D. P. Fenning, “Quantitative Determination of Moisture Content in Modules by Short-Wave Infrared Reflectometry,” *IEEE J. Photovoltaics*, vol. 9, no. 6, pp. 1748–1753, 2019.